Chiral spin liquid with spinon Fermi surfaces in the spin-1/2 triangular Heisenberg model

Shou-Shu Gong, Wayne Zheng, Mac Lee, Yuan-Ming Lu, and D. N. Sheng

Phys. Rev. B **100**, 241111 — Published 16 December 2019

DOI: 10.1103/PhysRevB.100.241111

Chiral spin liquid with spinon Fermi surfaces in spin-$1/2$ triangular Heisenberg model

Shou-Shu Gong[1], Wayne Zheng[2], Mac Lee[3,4], Yuan-Ming Lu[2], D. N. Sheng[3]
[1]*Department of Physics, Beihang University, Beijing 100191, China*
[2]*Department of Physics, Ohio State University, Columbus, Ohio 43210, USA*
[3]*Department of Physics and Astronomy, California State University, Northridge, CA 91330, USA*
[4]*Department of Physics, University of California, San Diego, CA 92093, USA*

We study the interplay of competing interactions in spin-$1/2$ triangular Heisenberg model through tuning the first- (J_1), second- (J_2), and third-neighbor (J_3) couplings. Based on large-scale density matrix renormalization group calculation, we identify a quantum phase diagram of the system and discover a new *gapless* chiral spin liquid (CSL) phase in the intermediate J_2 and J_3 regime. This CSL state spontaneously breaks time-reversal symmetry with finite scalar chiral order, and it has gapless excitations implied by a vanishing spin triplet gap and a finite central charge on the cylinder. Moreover, the central charge grows rapidly with the cylinder circumference, indicating emergent spinon Fermi surfaces. To understand the numerical results we propose a parton mean-field spin liquid state, the $U(1)$ staggered flux state, which breaks time-reversal symmetry with chiral edge modes by adding a Chern insulator mass to Dirac spinons in the $U(1)$ Dirac spin liquid. This state also breaks lattice rotational symmetries and possesses two spinon Fermi surfaces driven by nonzero J_2 and J_3, which naturally explains the numerical results. To our knowledge, this is the first example of a gapless CSL state with coexisting spinon Fermi surfaces and chiral edge states, demonstrating the rich family of novel phases emergent from competing interactions in triangular-lattice magnets.

PACS numbers: 73.43.Nq, 75.10.Jm, 75.10.Kt

Introduction. Quantum spin liquids (QSLs) are novel quantum phases of matter, which do not exhibit any symmetry-breaking orders even at zero temperature[1–3] but feature long-range entanglement and fractionalized excitations[4–7]. QSLs have been studied extensively in the past few decades, due to their important role in understanding strongly correlated materials and potential application in topological quantum computation[8–12]. While gapped QSLs have been classified and characterized systematically, there is much less understanding on gapless QSLs and how they could be realized in materials. Although a gapless QSL with Dirac cones of spinons has been shown to exist in the exactly soluble Kitaev model[12], so far there is no definitive evidence that a Dirac spin liquid has been realized in any magnetic materials[2,13]. A more exotic state is the gapless QSL with spinon Fermi surfaces (SFSs)[14–16]. Such a QSL has an extensive number of low-energy excitations, and was shown to be stabilized by four-spin ring-exchange couplings that can arise from strong charge fluctuations in weak Mott insulators[17–21].

Experimentally, many QSL candidate materials fall into the family of layered spin-$1/2$ magnets on the triangular lattice, such as the organic salts[22–26] and the transition metal dichalcogenides[27–30]. Specific heat and thermal transport measurements point towards the presence of extensive mobile gapless spin excitations, which appear to be consistent with a gapless QSL with SFSs[24,26,28]. These materials are considered to be weak Mott insulators with strong charge fluctuations, which may induce such gapless QSL behaviors[17–21]. However, a direct study on the triangular Hubbard model suggests a possible gapped chiral spin liquid (CSL) phase in the intermediate U region[31]. Therefore, a clear theoretical understanding on the mechanism to realize gapless QSLs in these layered quasi-two-dimensional magnets is still lacking.

Another route to QSL is through competing interactions between different neighboring sites, such as the kagome compound kapellasite[32] and J_1-J_2-J_3 kagome model[33,34]. Recently, competing interactions have also been found essential to understand possible QSLs in the triangular-lattice rare-earth compounds[35–39] and delafossite oxides[40–43]. Indeed, a QSL phase has been found in the spin-$1/2$ J_1-J_2 triangular Heisenberg model (THM) although its nature has not been established[44–51]. Therefore, understanding how QSL phases emerge from competing interactions is an important issue in order to discover new QSL materials[52–54].

In this Rapid communication, we systematically study the spin-$1/2$ J_1-J_2-J_3 THM using density-matrix renormalization group (DMRG) method and the parton construction. The model Hamiltonian is given as

$$H = J_1 \sum_{\langle i,j\rangle} \mathbf{S}_i \cdot \mathbf{S}_j + J_2 \sum_{\langle\langle i,j\rangle\rangle} \mathbf{S}_i \cdot \mathbf{S}_j + J_3 \sum_{\langle\langle\langle i,j\rangle\rangle\rangle} \mathbf{S}_i \cdot \mathbf{S}_j, \quad (1)$$

where J_1, J_2, J_3 are the first-, second-, and third NN interactions as shown in the inset of Fig. 1(a). We choose $J_1 = 1.0$ as the energy scale. In the coupling range $0 \leq J_2/J_1 \leq 0.7, 0 \leq J_3/J_1 \leq 0.4$, besides the previously found J_1-J_2 spin liquid and different magnetic orders, we identify a new gapless CSL phase as shown in Fig. 1(a). This CSL state spontaneously breaks time-reversal symmetry (TRS) with a finite scalar chiral order. We also observe spin pumping upon flux insertion, similar to the charge pumping in Laughlin-type fractional quantum Hall states, indicative of a chiral edge mode, which is further confirmed by the entanglement spectrum. Finite-size scaling of spin triplet gap on the square-like clusters shows a vanished spin gap. The gapless nature is further supported by the bipartite entanglement entropy, which exhibits a logarithmic correction of the area law versus subsystem length, leading to a finite central charge. The central charge grows with the cylinder circumference consistent with a QSL with emergent SFSs. We propose a staggered flux state in the Abrikosov-fermion representation of spin-$1/2$ opera-

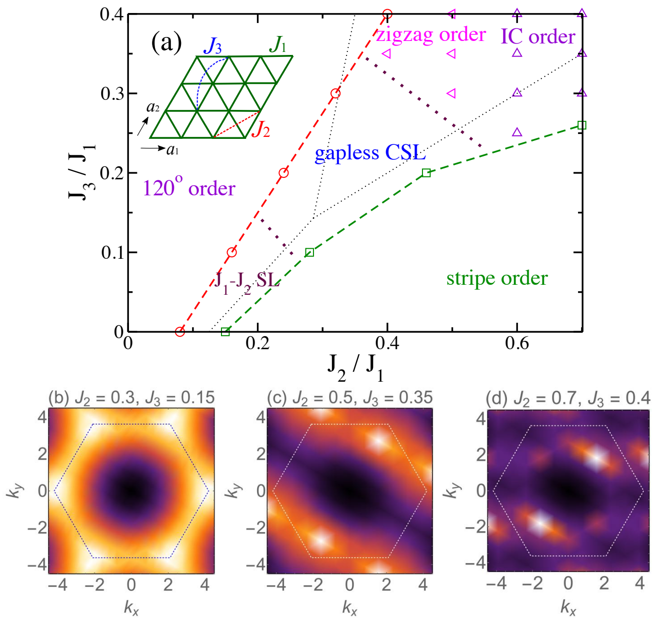

FIG. 1. Quantum phase diagram of spin-1/2 J_1-J_2-J_3 THM. The inset shows the model on the YC geometry. We find a 120^0 order, a stripe order, a zigzag order, an incommensurate (IC) order, and a gapless chiral spin liquid (CSL) phase in the neighbor of the previously found J_1-J_2 spin liquid (SL) phase. The colored dotted-lines are schematic phase boundaries, and the black dotted-lines are the classical phase boundaries of the 120^0, stripe, and zigzag orders. Static spin structure factors of the gapless CSL (b), the zigzag state (c), and the incommensurate state (d) on the YC8 cylinder.

tors, which explains the coexistence of chiral edge mode and SFSs observed in this gapless CSL.

We study the system by using DMRG with $SU(2)$ symmetry[55,56]. We use cylinder geometry with periodic boundary conditions along circumference direction and open boundary conditions along extended direction. The lattice vectors are defined as $\mathbf{a}_1 = (1, 0)$ and $\mathbf{a}_2 = (\frac{1}{2}, \frac{\sqrt{3}}{2})$. Two geometries named YC and XC cylinders are studied, both having extended direction along $\mathbf{a}_1$. For the YC and XC cylinders, circumference direction is along $\mathbf{a}_2$ and perpendicular to $\mathbf{a}_1$, respectively. The cylinders are denoted as YC$L_y - L_x$ and XC$L_y - L_x$ with L_y and L_x being the numbers of sites along circumference and extended directions. We study the systems with $L_y = 5 - 12$ by keeping up to 8000 $SU(2)$ states (equivalent to about 24000 $U(1)$ states) to obtain accurate results with truncation error less than 10^{-5} in most calculations.

Quantum phase diagram. We demonstrate the quantum phase diagram in Fig. 1(a). With growing J_2 and J_3, we find different magnetically ordered phases and QSL phases. In Fig. 1(a), the black dotted lines denote the classical phase boundaries of the 120^0, stripe, and zigzag orders. We also find an incommensurate (IC) magnetic order in the neighbor of the zigzag order, consistent with previous spin-wave calculations[52]. The incommensurate order might be considered as the zigzag order with an incommensurate modulation (see Supplemental Material[57]). In the presence of quantum fluctuations, we find a new gapless CSL phase near the triple point

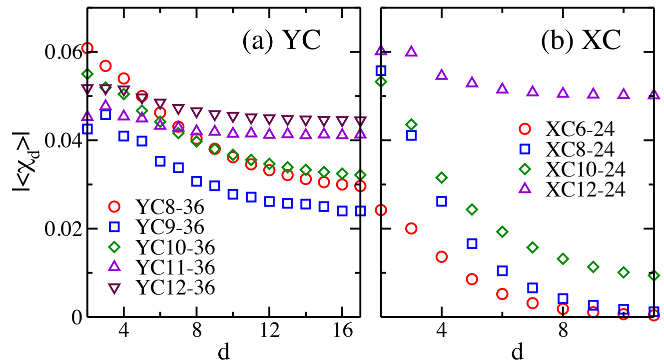

FIG. 2. Finite scalar chiral order of the CSL state at $J_2 = 0.3, J_3 = 0.15$. (a) and (b) are the scalar chiral order measured from the boundary to the bulk on the YC and XC cylinders. The scalar chiral order $\langle\chi\rangle = \langle \mathbf{S}_1 \cdot (\mathbf{S}_2 \times \mathbf{S}_3)\rangle$ is defined for the three spins $\mathbf{S}_i$ $(i = 1, 2, 3)$ for each triangle, and d is the distance of the triangle from the edge. The chiral orders of all the triangles have the same chiral direction.

of the classical orders, which sits at the neighbor of the J_1-J_2 SL. By computing spin and dimer correlation functions, we find featureless spin and dimer structure factors that indicate the absence of spin and dimer orders in the CSL state[57]. Next, we further characterize the nature of this new CSL state.

Spontaneous time-reversal symmetry breaking. To detect spontaneous TRS breaking, we use complex-valued wavefunction, which has been applied in DMRG to find chiral ground states in different systems[33,58]. If TRS is spontaneously broken, the system is featured by finite scalar chiral order $\langle\chi\rangle = \langle \mathbf{S}_1 \cdot (\mathbf{S}_2 \times \mathbf{S}_3)\rangle$, where $\mathbf{S}_i$ $(i = 1, 2, 3)$ label the three spins on each triangle. On the YC cylinder with both even and odd L_y, we find a nonzero chiral order in the bulk of cylinder with a large circumference, as shown in Fig. 2(a) for $J_2 = 0.3, J_3 = 0.15$. In these states, the chiral orders of all the up- and down-triangles have the same sign, and the chiral order grows more robust as the circumference increases. On the XC cylinder shown in Fig. 2(b), the chiral order vanishes in the bulk for small circumference but becomes stable on the wide XC12 cylinder. Combining these results we conclude a CSL state with spontaneous TRS breaking.

Spin triplet gap and entanglement characterization. We calculate the spin triplet gap by obtaining the ground state (in the $S = 0$ sector) on long cylinder and then sweeping the $S = 1$ sector for the middle N_x columns[59], which gives the gap of the middle $N_x \times L_y$ system. We find that the gap versus $1/N_x$ shows length dependence[57]. To estimate the gap in the 2D limit and avoid 1D physics, we extrapolate the gap data of the square-like clusters as shown in Fig. 3(a). The gap drops fast as a function of $1/L_y$ and smoothly scales to zero, suggesting gapless spin-triplet excitations.

Furthermore, we study entanglement entropy versus subsystem length l_x by cutting the cylinder into two parts. Since the real-valued wavefunction is a superposition of the two chiral states with opposite chiralities, it has a higher entanglement entropy and is harder to converge to; thus we also use complex-valued wavefunction to compute entanglement entropy. As shown in Fig. 3(b) for $J_2 = 0.3, J_3 = 0.15$

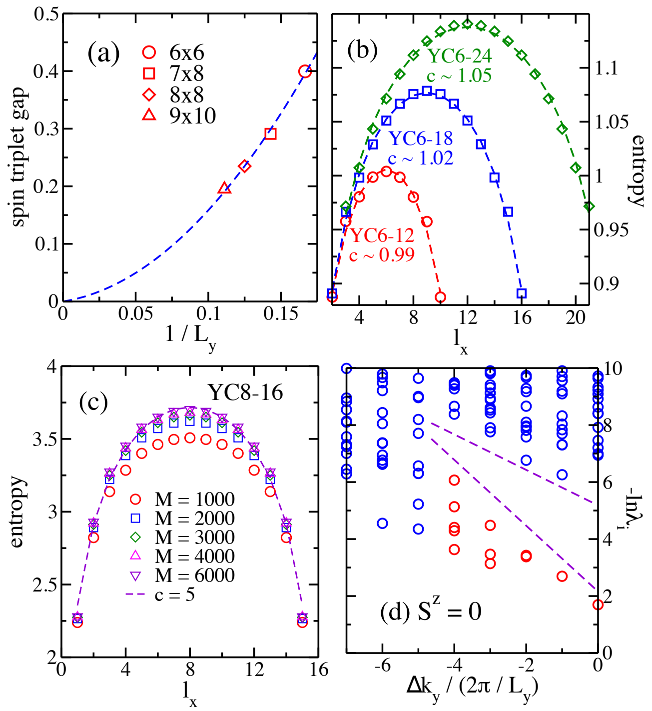

FIG. 3. (a) Size scaling of the spin triplet gap obtained on the square-like clusters. (b) Entanglement entropy versus subsystem length l_x on the YC6 cylinders with different L_x. (c) Entanglement entropy on the YC8-16 cylinder by keeping different $SU(2)$ state numbers. The dash lines denote the fitting of entropy following the formula $S(l_x) = (c/6)\ln[(L_x/\pi)\sin(l_x\pi/L_x)] + g$, giving central charge $c \simeq 1$ for the YC6 cylinder and $c \simeq 5$ for the YC8-16 cylinder. (d) Entanglement spectrum labeled by the quantum numbers total spin $S^z = 0$ and relative momentum along the y direction Δk_y. λ_i is the eigenvalue of reduced density matrix. The red circles denote the near degenerate pattern $\{1, 1, 2, 3, 5\}$ of the low-lying spectrum.

on the YC6 cylinder, the entropy shows a logarithmic correction of the area law and follows the behavior $S(l_x) = (c/6)\ln[(L_x/\pi)\sin(l_x\pi/L_x)] + g$[60], where $S(l_x)$ is the bipartite entanglement entropy, c is the central charge, and g is a non-universal constant. The YC6 cylinders with different L_x give a consistent central charge $c \simeq 1$. For the YC8 cylinder, we choose $L_x = 16$ (the entropy for larger L_x is much harder to converge and we show the results for $L_x = 24$ in Supplemental Material[57], which are consistent with the fitted central charge $c = 5$). As shown in Fig. 3(c), the entropy continues to grow with kept state number and converges very well by keeping 6000 $SU(2)$ states, giving a large central charge of $c \simeq 5$. The finite central charge supports the gapless nature of the CSL state. Once a 2D quantum state is confined to a 1D cylinder, the finite circumference quantizes the momentum around the cylinder. The central charge of the 1D cylinder needs to sum over contributions from all quantized momenta. Take the $U(1)$ Dirac spin liquid for example, the cylinder central charge $c = 2 - 1 = 1$ if the quantized momenta for each spin species only cross one Dirac cone, where the extra -1 accounts for the $U(1)$ gauge field fluctuations which gaps out the total spinon density fluctuation[57,61]. Similarly $c \leq 3$ if the quantized momenta cross two Dirac cones (for each spin species), which is an upper bound for the central charge on a cylinder of any L_y. The large central charge we found from DMRG is therefore inconsistent with the $U(1)$ Dirac spin liquid on triangular lattice[44,45,50], but provides a strong evidence supporting emergent SFSs[14,15,18,19]. Now that each pair of crossings (one right mover and one left mover) between the quantized momenta and the SFSs contributes a unit of central charge, the total central charge of SFSs generally grows with L_y, with an upper bound of $c \leq N_w - 1$ where $2N_w$ is the total number of crossings[57].

For gapped CSL states, entanglement spectrum has a one-to-one correspondence with physical edge spectrum[62]. Interestingly, for this gapless CSL state entanglement spectrum also shows a quasi-degenerate group of levels with the counting $\{1, 1, 2, 3, 5, \cdots\}$ agreeing with chiral $SU(2)_1$ conformal field theory[63], as shown in Fig. 3(d). This may be the first example of such novel states for interacting system, which demonstrates similar edge physics as the non-interacting $p+ip$ chiral superconductor with a gapless bulk spectrum[64,65].

The staggered flux state. To understand the DMRG results, we propose a staggered flux state, whose mean-field ansatz is constructed in the Abrikosov-fermion representation of spin-1/2 operators[66]

$$\mathbf{S}_i = \frac{1}{4}\mathrm{Tr}\left(\psi_i^\dagger \psi_i \boldsymbol{\sigma}^T\right), \quad \psi_i = \begin{pmatrix} f_{i,\uparrow} & f_{i,\downarrow} \\ f_{i,\downarrow}^\dagger & -f_{i,\uparrow}^\dagger \end{pmatrix} \tag{2}$$

The Heisenberg Hamiltonian $H = \sum_{\langle ij\rangle} J_{ij}\mathbf{S}_i \cdot \mathbf{S}_j$ is decoupled into the mean-field form as

$$H_{\mathbf{MF}} = \frac{1}{8}\sum_{ij} J_{ij}\mathrm{Tr}\left(\psi_i^\dagger u_{ij}\psi_j + h.c.\right) + \frac{1}{8}\sum_{ij} J_{ij}\mathrm{Tr}\left(u_{ij}^\dagger u_{ij}\right)$$

with the mean-field amplitude $u_{ij} = \langle \psi_i \psi_j^\dagger \rangle = u_{ij}^\dagger$. In the $U(1)$ QSL states all spinon pairing terms will vanish and thus

$$u_{ij} = \begin{pmatrix} -\bar{\chi}_{ij} & 0 \\ 0 & \chi_{ij} \end{pmatrix}, \tag{3}$$

where $\chi_{ij} = \sum_\alpha \langle f_{i,\alpha}^\dagger f_{j,\alpha}\rangle = \bar{\chi}_{ji}$. Then the mean-field ansatz can be simplified as

$$H_{\mathbf{MF}} = \frac{J}{4}\sum_{\langle ij\rangle}\sum_{\alpha}\left(-\bar{\chi}_{ij} f_{i,\alpha}^\dagger f_{j,\alpha} + h.c.\right) + \frac{J}{4}\sum_{\langle ij\rangle}\left(|\chi_{ij}|^2\right)$$

where the mean-field ground state is at half-filling due to the single-occupancy constraint on the parton Hilbert space

$$\sum_{\alpha=\uparrow,\downarrow} f_{i\alpha}^\dagger f_{i\alpha} = 1, \quad \forall\, i. \tag{4}$$

We consider a $U(1)$ spin liquid known as the staggered flux state[67–69], where fermionic spinons transform under translations as follows

$$f_{\mathbf{r},\alpha} \xrightarrow{T_2} (-)^{r_1} f_{\mathbf{r}+\mathbf{a}_2,\alpha}^\dagger, \quad f_{\mathbf{r},\alpha} \xrightarrow{T_1} f_{\mathbf{r}+\mathbf{a}_1,\alpha}. \tag{5}$$

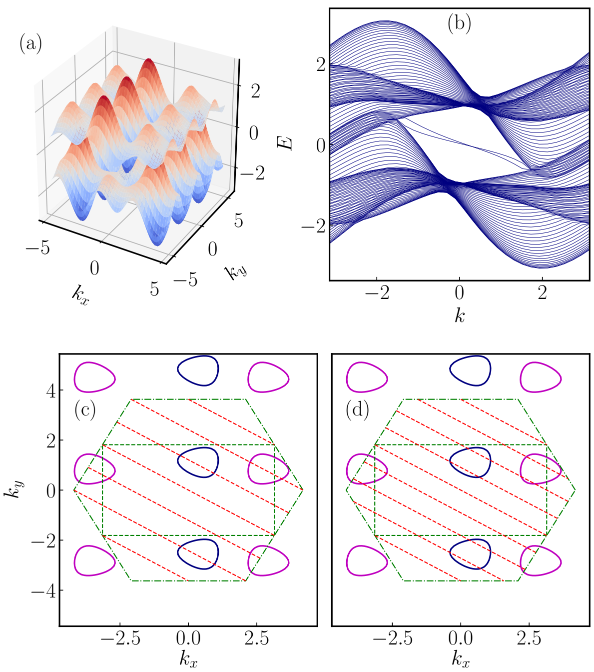

FIG. 4. Mean-field ansatz of the staggered flux state with up to third NN mean-field amplitudes. (a) Spinon dispersion. (b) Edge spectrum on a cylinder geometry. (c) and (d) show how the 1d channels with quantized momentum $k_2 = \frac{2\pi}{L_y} l_2,\ l_2 \in \mathbb{Z}$ cross the spinon Fermi surfaces (SFSs) on finite YC cylinders with $L_y = 6, 8$. The dotted rectangle is the reduced Brillouin zone due to the doubling of unit cell in the mean-field ansatz. Pink and blue circles denote hole- and particle-like SFSs respectively.

Although the mean-field ansatz doubles the unit cell (along $\mathbf{a}_2$ direction), the projected wavefunction preserves the lattice translation symmetries by $\mathbf{a}_{1,2}$.

Since the spin model has couplings up to the 3rd NN sites, we consider the symmetry-allowed mean-field ansatz with hopping terms up to the 3rd NN, which are shown in Supplemental Material[57]. The NN hopping ansatz reduces to the π-flux $U(1)$ QSL state[50] in the case of $\phi_1 = \phi_2 = \pi/2$ (ϕ_1, ϕ_2 are the phases of the NN hoppings), with a pair of Dirac spinons at half filling for each spin species. The 2nd and 3rd NN hoppings can open up a direct gap at each Dirac cone, leading to a Chern number $C = \pm 1$ of the lower spinon band and the chiral edge states shown in Fig. 4(b). Meanwhile the 3rd NN hoppings can break the degeneracy of two Dirac cones, giving rise to one particle-like SFS around one Dirac point (blue in Figs. 4(c-d)) and a hole-like SFS around the other Dirac point (pink in Figs. 4(c-d)). Due to single-occupancy constraint Eq. (4), the particle-like SFS and hole-like SFS are perfectly compensated at half filling. Choosing mean-field parameters as $\chi = 1.0, \phi_1 = \phi_2 = \pi/2, \lambda = 1.0, \varphi_1 = \varphi_2 = \varphi_3 = 0, \rho = 3.0, \gamma_1 = \gamma_2 = \gamma_3 = \pi/2$[57], the mean-field dispersion and edge spectrum of fermionic spinons are shown in Figs. 4(a-b).

For further comparison with DMRG, we follow the YC cylinder geometry with quantized momentum $k_2 = 2\pi l_2/L_y$ along $\mathbf{b}_2$ direction. In Fig. 4(c) and (d) we depict how the 1D channels with quantized momenta $k_2 = 2\pi l_2/L_y$ intersect with the two SFSs in the reduced Brillouin zone of the staggered flux state. On the YC6 cylinder, as shown in Fig. 4(c), there are $N_w = 2 \times 2 = 4$ pairs of gapless 1D modes crossing the SFSs (counting both spin species), constraining the central charge to be $c \leq N_w - 1 = 3$. On the YC8 cylinder, as shown in Fig. 4(d), there are $N_w = 2 \times 4 = 8$ pairs of gapless 1D modes crossing the SFSs, restricting the central charge as $c \leq N_w - 1 = 7$. This is consistent with the observed $c \approx 1$ on YC6-24 cylinder (Fig. 3(b)) and $c \approx 5$ on YC8-16 cylinder (Fig. 3(c)). Note that the number $N_w - 1$ only bound the actual central charge from above, since symmetric backscatterings between these gapless 1D channels can further reduce the total central charge from $N_w - 1$[57].

Discussion. The spin structure factor of the gapless CSL phase in Fig. 1(b) resembles that of the $U(1)$ Dirac spin liquid[45]. Specifically, it exhibits high intensities on the edge and at the corner of the hexagonal Brillouin zone, which are associated with fermion bilinears and monopoles respectively in the $U(1)$ Dirac spin liquid[70,71]. This suggests the proximity of the gapless CSL to the $U(1)$ Dirac state, which is indeed the case for the proposed staggered flux state. We have also studied the phase transition from the J_1-J_2 SL phase to the gapless CSL phase. The ground-state energy versus couplings is very smooth, suggesting a possible continuous phase transition[57]. Interestingly, in the J_1-J_2 SL entanglement entropy also shows a logarithmic correction of the area law, which leads to a finite central charge[57]. A new insight for its ground state could be a gapless spin liquid with SFSs but preserving TRS, which we leave for future work.

Summary. We have studied the spin-1/2 J_1-J_2-J_3 THM by extensive DMRG calculations. We identify a CSL state spontaneously breaking TRS, featuring a chiral edge mode and spin pumping upon flux insertion. The vanishing spin triplet gap and finite central charge reveal the gapless nature of this state. The central charge which grows with system circumference further indicates emergent SFSs. While the competing J_2, J_3 couplings lead to a gapped CSL on kagome lattice[34,72], they induce a gapless CSL on triangular lattice. On the mean-field level we propose a staggered flux state driven by the J_2, J_3 couplings, which breaks TRS and forms SFS, providing a theoretical understanding for such a novel gapless phase. The discovery of this gapless CSL reveals the novel possibility for the coexistence of chiral edge modes and SFSs in a gapless QSL, emergent from competing interactions in a frustrated two-dimensional magnet.

Note added. After completion of this work, we became aware of a work by Shijie Hu et al.[73], who studied the J_1-J_2 spin liquid. Compared to their work, our work focuses on the J_1-J_2-J_3 model and found a staggered flux state driven by further-neighbor interactions.

ACKNOWLEDGMENTS

We would like to thank Olexei I. Motrunich, Tao Li, and Yuan Wan for extensive discussions. S.S.G. is supported by the National Natural Science Foundation of China Grants (11874078, 11834014) and the Fundamental Research Funds for the Central Universities. M.L. is supported by the National Science Foundation through PREM Grant DMR-1828019. D.N.S. is supported by the U.S. Department of Energy, Office of Basic Energy Sciences under Grant No. DE-FG02-06ER46305. W.Z. and Y.M.L. are supported by National Science Foundation under award number DMR-1653769.

---

[1] L. Balents, "Spin liquids in frustrated magnets," Nature (London) **464**, 199–208 (2010).

[2] Lucile Savary and Leon Balents, "Quantum spin liquids: a review," Reports on Progress in Physics **80**, 016502 (2016).

[3] Yi Zhou, Kazushi Kanoda, and Tai-Kai Ng, "Quantum spin liquid states," Rev. Mod. Phys. **89**, 025003 (2017).

[4] X. G. Wen, "Mean-field theory of spin-liquid states with finite energy gap and topological orders," Phys. Rev. B **44**, 2664–2672 (1991).

[5] T. Senthil and Matthew P. A. Fisher, "Z_2 gauge theory of electron fractionalization in strongly correlated systems," Phys. Rev. B **62**, 7850–7881 (2000).

[6] T. Senthil and Matthew P. A. Fisher, "Fractionalization in the cuprates: Detecting the topological order," Phys. Rev. Lett. **86**, 292–295 (2001).

[7] Xiao-Gang Wen, "Topological order: From long-range entangled quantum matter to a unified origin of light and electrons," ISRN Condensed Matter Physics **2013**, Article ID 198710 (2013).

[8] P. W. Anderson, "Resonating valence bonds: A new kind of insulator?" Mater. Res. Bull. **8**, 153 (1973).

[9] N. Read and Subir Sachdev, "Large-n expansion for frustrated quantum antiferromagnets," Phys. Rev. Lett. **66**, 1773–1776 (1991).

[10] Subir Sachdev, "Kagome and triangular-lattice heisenberg antiferromagnets: Ordering from quantum fluctuations and quantum-disordered ground states with unconfined bosonic spinons," Phys. Rev. B **45**, 12377–12396 (1992).

[11] Patrick A. Lee, Naoto Nagaosa, and Xiao-Gang Wen, "Doping a mott insulator: Physics of high-temperature superconductivity," Rev. Mod. Phys. **78**, 17–85 (2006).

[12] A. Kitaev, "Anyons in an exactly solved model and beyond," Annals of Physics **321**, 2–111 (2006).

[13] M. Hermanns, I. Kimchi, and J. Knolle, "Physics of the kitaev model: Fractionalization, dynamic correlations, and material connections," Annual Review of Condensed Matter Physics **9**, 17–33 (2018).

[14] L. B. Ioffe and A. I. Larkin, "Gapless fermions and gauge fields in dielectrics," Phys. Rev. B **39**, 8988–8999 (1989).

[15] Naoto Nagaosa and Patrick A. Lee, "Normal-state properties of the uniform resonating-valence-bond state," Phys. Rev. Lett. **64**, 2450–2453 (1990).

[16] Patrick A. Lee and Naoto Nagaosa, "Gauge theory of the normal state of high-t_c superconductors," Phys. Rev. B **46**, 5621–5639 (1992).

[17] G. Misguich, C. Lhuillier, B. Bernu, and C. Waldtmann, "Spin-liquid phase of the multiple-spin exchange hamiltonian on the triangular lattice," Phys. Rev. B **60**, 1064–1074 (1999).

[18] Olexei I. Motrunich, "Variational study of triangular lattice spin-12 model with ring exchanges and spin liquid state in κ-(et)$_2$cu$_2$(cn)$_3$," Phys. Rev. B **72**, 045105 (2005).

[19] D. N. Sheng, Olexei I. Motrunich, and Matthew P. A. Fisher, "Spin bose-metal phase in a spin-$\frac{1}{2}$ model with ring exchange on a two-leg triangular strip," Phys. Rev. B **79**, 205112 (2009).

[20] Matthew S. Block, D. N. Sheng, Olexei I. Motrunich, and Matthew P. A. Fisher, "Spin bose-metal and valence bond solid phases in a spin-$1/2$ model with ring exchanges on a four-leg triangular ladder," Phys. Rev. Lett. **106**, 157202 (2011).

[21] Wen-Yu He, Xiao Yan Xu, Gang Chen, K. T. Law, and Patrick A. Lee, "Spinon fermi surface in a cluster mott insulator model on a triangular lattice and possible application to $1t\mathrm{-tas}_2$," Phys. Rev. Lett. **121**, 046401 (2018).

[22] Y. Shimizu, K. Miyagawa, K. Kanoda, M. Maesato, and G. Saito, "Spin liquid state in an organic mott insulator with a triangular lattice," Phys. Rev. Lett. **91**, 107001 (2003).

[23] Y. Kurosaki, Y. Shimizu, K. Miyagawa, K. Kanoda, and G. Saito, "Mott transition from a spin liquid to a fermi liquid in the spin-frustrated organic conductor κ-(et)$_2$cu$_2$(cn)$_3$," Phys. Rev. Lett. **95**, 177001 (2005).

[24] Satoshi Yamashita, Yasuhiro Nakazawa, Masaharu Oguni, Yugo Oshima, Hiroyuki Nojiri, Yasuhiro Shimizu, Kazuya Miyagawa, and Kazushi Kanoda, "Thermodynamic properties of a spin-1/2 spin-liquid state in a κ-type organic salt," Nature Physics **4**, 459–462 (2008).

[25] Minoru Yamashita, Norihito Nakata, Yuichi Kasahara, Takahiko Sasaki, Naoki Yoneyama, Norio Kobayashi, Satoshi Fujimoto, Takasada Shibauchi, and Yuji Matsuda, "Thermal-transport measurements in a quantum spin-liquid state of the frustrated triangular magnet-(bedt-ttf) 2cu2 (cn) 3," Nature Physics **5**, 44–47 (2009).

[26] Minoru Yamashita, Norihito Nakata, Yoshinori Senshu, Masaki Nagata, Hiroshi M Yamamoto, Reizo Kato, Takasada Shibauchi, and Yuji Matsuda, "Highly mobile gapless excitations in a two-dimensional candidate quantum spin liquid," Science **328**, 1246–1248 (2010).

[27] K. T. Law and Patrick A. Lee, "1t-tas2 as a quantum spin liquid," Proceedings of the National Academy of Sciences **114**, 6996–7000 (2017), http://www.pnas.org/content/114/27/6996.full.pdf.

[28] Y. J. Yu, Y. Xu, L. P. He, M. Kratochvilova, Y. Y. Huang, J. M. Ni, Lihai Wang, Sang-Wook Cheong, Je-Geun Park, and S. Y. Li, "Heat transport study of the spin liquid candidate $1t\mathrm{-tas}_2$," Phys. Rev. B **96**, 081111 (2017).

[29] A. Ribak, I. Silber, C. Baines, K. Chashka, Z. Salman, Y. Dagan, and A. Kanigel, "Gapless excitations in the ground state of $1t\mathrm{-tas}_2$," Phys. Rev. B **96**, 195131 (2017).

[30] Martin Klanjšek, Andrej Zorko, Rok Žitko, Jernej Mravlje, Zvonko Jagličić, Pabitra Kumar Biswas, Peter Prelovšek, Dragan Mihailovic, and Denis Arčon, "A high-temperature quantum spin liquid with polaron spins," Nature Physics **13**, 1130 EP – (2017).

[31] Aaron Szasz, Johannes Motruk, Michael P. Zaletel, and Joel E. Moore, "Observation of a chiral spin liquid phase of the Hubbard model on the triangular lattice: a density matrix renormalization group study," arXiv e-prints , arXiv:1808.00463 (2018), arXiv:1808.00463 [cond-mat.str-el].

[32] B. Fåk, E. Kermarrec, L. Messio, B. Bernu, C. Lhuillier, F. Bert, P. Mendels, B. Koteswararao, F. Bouquet, J. Ollivier, A. D. Hillier, A. Amato, R. H. Colman, and A. S. Wills, "Kapellasite: A kagome quantum spin liquid with competing interactions," Phys. Rev. Lett. **109**, 037208 (2012).

[33] Shou-Shu Gong, Wei Zhu, and D. N. Sheng, "Emergent chiral spin liquid: fractional quantum hall effect in a kagome heisenberg

model," Scientific reports **4**, 6317 (2014).

[34] Shou-Shu Gong, Wei Zhu, Leon Balents, and D. N. Sheng, "Global phase diagram of competing ordered and quantum spin-liquid phases on the kagome lattice," Phys. Rev. B **91**, 075112 (2015).

[35] Joseph AM Paddison, Marcus Daum, Zhiling Dun, Georg Ehlers, Yaohua Liu, Matthew B Stone, Haidong Zhou, and Martin Mourigal, "Continuous excitations of the triangular-lattice quantum spin liquid ybmggao4," Nature Physics (2016).

[36] Zhenyue Zhu, P. A. Maksimov, Steven R. White, and A. L. Chernyshev, "Topography of spin liquids on a triangular lattice," Phys. Rev. Lett. **120**, 207203 (2018).

[37] Xinshu Zhang, Fahad Mahmood, Marcus Daum, Zhiling Dun, Joseph A. M. Paddison, Nicholas J. Laurita, Tao Hong, Haidong Zhou, N. P. Armitage, and Martin Mourigal, "Hierarchy of exchange interactions in the triangular-lattice spin liquid $\mathrm{ybmggao}_4$," Phys. Rev. X **8**, 031001 (2018).

[38] Yuesheng Li, Gang Chen, Wei Tong, Li Pi, Juanjuan Liu, Zhaorong Yang, Xiaoqun Wang, and Qingming Zhang, "Rare-earth triangular lattice spin liquid: A single-crystal study of $\mathrm{ybmggao}_4$," Phys. Rev. Lett. **115**, 167203 (2015).

[39] Yao Shen, Yao-Dong Li, H. C. Walker, P. Steffens, M. Boehm, Xiaowen Zhang, Shoudong Shen, Hongliang Wo, Gang Chen, and Jun Zhao, "Fractionalized excitations in the partially magnetized spin liquid candidate ybmggao4," Nature Communications **9**, 4138 (2018).

[40] T. Kimura, J. C. Lashley, and A. P. Ramirez, "Inversion-symmetry breaking in the noncollinear magnetic phase of the triangular-lattice antiferromagnet CuFeo_2," Phys. Rev. B **73**, 220401 (2006).

[41] F. Ye, J. A. Fernandez-Baca, R. S. Fishman, Y. Ren, H. J. Kang, Y. Qiu, and T. Kimura, "Magnetic interactions in the geometrically frustrated triangular lattice antiferromagnet cufeo_2," Phys. Rev. Lett. **99**, 157201 (2007).

[42] H. Kadowaki, H. Kikuchi, and Y. Ajiro, "Neutron powder diffraction study of the two-dimensional triangular lattice antiferromagnet cucro 2," Journal of Physics: Condensed Matter **2**, 4485 (1990).

[43] S. Seki, Y. Onose, and Y. Tokura, "Spin-driven ferroelectricity in triangular lattice antiferromagnets $a\mathrm{cro}_2$ ($a = \mathrm{Cu}$, ag, li, or na)," Phys. Rev. Lett. **101**, 067204 (2008).

[44] Ryui Kaneko, Satoshi Morita, and Masatoshi Imada, "Gapless spin-liquid phase in an extended spin 1/2 triangular heisenberg model," Journal of the Physical Society of Japan **83** (2014).

[45] Yasir Iqbal, Wen-Jun Hu, Ronny Thomale, Didier Poilblanc, and Federico Becca, "Spin liquid nature in the heisenberg $j_1 - j_2$ triangular antiferromagnet," Phys. Rev. B **93**, 144411 (2016).

[46] P. H. Y. Li, R. F. Bishop, and C. E. Campbell, "Quasiclassical magnetic order and its loss in a spin-$\frac{1}{2}$ heisenberg antiferromagnet on a triangular lattice with competing bonds," Phys. Rev. B **91**, 014426 (2015).

[47] Zhenyue Zhu and Steven R. White, "Spin liquid phase of the $s = \frac{1}{2}$ $j_1 - j_2$ heisenberg model on the triangular lattice," Phys. Rev. B **92**, 041105 (2015).

[48] Wen-Jun Hu, Shou-Shu Gong, Wei Zhu, and D. N. Sheng, "Competing spin-liquid states in the spin-$\frac{1}{2}$ heisenberg model on the triangular lattice," Phys. Rev. B **92**, 140403 (2015).

[49] W. Zheng, J.-W. Mei, and Y. Qi, "Classification and Monte Carlo study of symmetric Z_2 spin liquids on the triangular lattice," ArXiv e-prints (2015), arXiv:1505.05351 [cond-mat.str-el].

[50] Yuan-Ming Lu, "Symmetric Z_2 spin liquids and their neighboring phases on triangular lattice," Phys. Rev. B **93**, 165113 (2016).

[51] S. N. Saadatmand and I. P. McCulloch, "Symmetry fractionalization in the topological phase of the spin-1/2 $j_1 - j_2$ triangular heisenberg model," Phys. Rev. B **94**, 121111 (2016).

[52] N.B. Ivanov and J. Richter, "Spiral phases in easy plane j1-j2-j3 triangular antiferromagnets," Journal of Magnetism and Magnetic Materials **140-144**, 1965 (1995), international Conference on Magnetism.

[53] N. Y. Yao, M. P. Zaletel, D. M. Stamper-Kurn, and A. Vishwanath, "A quantum dipolar spin liquid," Nature Physics **14**, 405–410 (2018).

[54] Jason Iaconis, Chunxiao Liu, Gbor B. Halsz, and Leon Balents, "Spin Liquid versus Spin Orbit Coupling on the Triangular Lattice," SciPost Phys. **4**, 003 (2018).

[55] Steven R. White, "Density matrix formulation for quantum renormalization groups," Phys. Rev. Lett. **69**, 2863–2866 (1992).

[56] IP McCulloch and M Gulácsi, "The non-abelian density matrix renormalization group algorithm," Europhysics Letters **57**, 852–858 (2002).

[57] See Supplemental Material for more details.

[58] W. Zhu, Shou-Shu Gong, Tian-Sheng Zeng, Liang Fu, and D. N. Sheng, "Interaction-driven spontaneous quantum hall effect on a kagome lattice," Phys. Rev. Lett. **117**, 096402 (2016).

[59] S. Yan, D. A. Huse, and S. R. White, "Spin-Liquid Ground State of the S = 1/2 Kagome Heisenberg Antiferromagnet," Science **332**, 1173 (2011).

[60] Pasquale Calabrese and John Cardy, "Entanglement entropy and quantum field theory," J. Stat. Mech.: Theor. Exp. **2004**, P06002 (2004).

[61] Scott D. Geraedts, Michael P. Zaletel, Roger S. K. Mong, Max A. Metlitski, Ashvin Vishwanath, and Olexei I. Motrunich, "The half-filled landau level: The case for dirac composite fermions," Science **352**, 197 (2016).

[62] Hui Li and F. D. M. Haldane, "Entanglement spectrum as a generalization of entanglement entropy: Identification of topological order in non-abelian fractional quantum hall effect states," Phys. Rev. Lett. **101**, 010504 (2008).

[63] Philippe Francesco, Pierre Mathieu, and David Sénéchal, *Conformal field theory* (Springer Science & Business Media, 2012).

[64] J. Dubail and N. Read, "Tensor network trial states for chiral topological phases in two dimensions and a no-go theorem in any dimension," Phys. Rev. B **92**, 205307 (2015).

[65] Didier Poilblanc, "Investigation of the chiral antiferromagnetic heisenberg model using projected entangled pair states," Phys. Rev. B **96**, 121118 (2017).

[66] A. A. Abrikosov, "Electron scattering on magnetic impurities in metals and anomalous resistivity effects," Physics **2**, 5–20 (1965).

[67] Xiao-Gang Wen, "Quantum orders and symmetric spin liquids," Phys. Rev. B **65**, 165113 (2002).

[68] Yao-Dong Li, Yuan-Ming Lu, and Gang Chen, "Spinon fermi surface $u(1)$ spin liquid in the spin-orbit-coupled triangular-lattice mott insulator $\mathrm{ybmggao}_4$," Phys. Rev. B **96**, 054445 (2017).

[69] Samuel Bieri, Claire Lhuillier, and Laura Messio, "Projective symmetry group classification of chiral spin liquids," Phys. Rev. B **93**, 094437 (2016).

[70] Xue-Yang Song, Chong Wang, Ashvin Vishwanath, and Yin-Chen He, "Unifying Description of Competing Orders in Two Dimensional Quantum Magnets," arXiv e-prints , arXiv:1811.11186 (2018), arXiv:1811.11186 [cond-mat.str-el].

[71] Xue-Yang Song, Yin-Chen He, Ashvin Vishwanath, and Chong Wang, "From spinon band topology to the symmetry quantum numbers of monopoles in Dirac spin liquids," arXiv e-prints , arXiv:1811.11182 (2018), arXiv:1811.11182 [cond-mat.str-el].

[72] Yin-Chen He, D. N. Sheng, and Yan Chen, "Chiral spin liquid in a frustrated anisotropic kagome heisenberg model," Phys. Rev. Lett. **112**, 137202 (2014).

[73] Shijie Hu, W. Zhu, Sebastian Eggert, and Yin-Chen He, "Dirac Spin Liquid on the Spin-1/2 Triangular Heisenberg Antiferromag-

net," arXiv e-prints , arXiv:1905.09837 (2019), arXiv:1905.09837 [cond-mat.str-el].